Relationships between the Brewer-Dobson circulation and the southern annular mode during austral summer in coupled chemistry-climate model simulations

Feng Li,[1] Paul A. Newman,[2] and Richard S. Stolarski[2]

Received 22 July 2009; revised 10 February 2010; accepted 19 February 2010; published 6 August 2010.

[1] The Brewer-Dobson circulation (BDC) is the mean meridional mass circulation in the stratosphere and the southern annular mode (SAM) is the prime variability pattern of the Southern Hemisphere extratropical troposphere. Motivated by previous studies showing that both the strengths of the BDC and the SAM have the largest trends in the austral summer in the recent past, this paper investigates the relationships between the BDC and the SAM using coupled chemistry-climate model simulations. The model results show that the strengthening of the BDC in the Southern Hemisphere during November–February (NDJF) is strongly projected onto the high index of the SAM. The trends in the BDC and the SAM are driven by Antarctic ozone depletion, which increases stratosphere-troposphere interactions through a delayed Antarctic vortex breakup. The prolonged persistence of stratospheric westerlies enhances upward propagation of tropospheric wave activity into the stratosphere and strengthens the BDC. The wave flux and westerly anomalies in the stratosphere in turn drive a SAM trend toward its high index. Model results also show that the BDC-SAM relationship is robust on the interannual time scale.

Citation: Li, F., P. A. Newman, and R. S. Stolarski (2010), Relationships between the Brewer-Dobson circulation and the southern annular mode during austral summer in coupled chemistry-climate model simulations, *J. Geophys. Res.*, *115*, D15106, doi:10.1029/2009JD012876.

1. Introduction

[2] The stratospheric mean meridional circulation, or the so-called Brewer-Dobson circulation (BDC), plays a crucial role in the distribution of ozone and other important trace species in the stratosphere [*Brewer*, 1949; *Dobson*, 1956]. The BDC consists of an upwelling branch in the tropics, poleward flows, and downwelling branches in the extratropics [*Andrews et al.*, 1987]. The forcing of the BDC is from Rossby and gravity wave breaking in the extratropical stratosphere, which deposits westward momentum in the stratosphere that drives a poleward flow [*Holton et al.*, 1995]. Because of mass continuity, poleward flow in the extratropical stratosphere induces rising motion in the tropics and sinking motion in the midlatitudes to high latitudes.

[3] *Butchart and Scaife* [2001] were the first to predict a strengthening of the BDC in response to an increase in greenhouse gases. Because an enhanced BDC has significant impacts on stratospheric transport, ozone recovery, and stratosphere-troposphere exchange, the strength of the BDC under global warming has been extensively investigated. Numerous middle-atmosphere model simulations have confirmed that an increase in the BDC is a robust model response to climate change [e.g., *Butchart et al.*, 2006]. Model results indicate that the acceleration of the BDC is caused by a stronger stratospheric wave forcing with contributions from both model resolved waves and parameterized gravity waves [*Butchart et al.*, 2006; *Li et al.*, 2008; *Garcia and Randel*, 2008; *McLandress and Shepherd*, 2009]. Several studies have linked the enhancement in the stratospheric wave driving to greenhouse gas (GHG) increase, sea surface temperature change, and stratospheric ozone depletion [*Butchart and Scaife*, 2001; *Li et al.*, 2008; *Garcia and Randel*, 2008; *Oman et al.*, 2009].

[4] Despite extensive studies of the BDC, there are still some outstanding dynamical questions. One important issue is whether and how changes in the BDC are connected to climate change in the troposphere, in particular, the annular modes. The annular modes are the leading variability in the extratropical troposphere at intraseasonal, interannual, and decadal time scales [*Thompson and Wallace*, 2000; *Thompson et al.*, 2000]. When the zonal-mean zonal wind in the stratosphere is weak westerly, the annular modes are coupled with the stratospheric circulation through active wave-mean flow interactions. During these active seasons, wind variability associated with the annular modes can modulate Rossby wave propagation into and within the stratosphere and hence can modulate the strength of the BDC. On the other hand,

[1]Goddard Earth Sciences and Technology Center, University of Maryland-Baltimore County, Baltimore, Maryland, USA.
[2]NASA Goddard Space Flight Center, Greenbelt, Maryland, USA.

Copyright 2010 by the American Geophysical Union.
0148-0227/10/2009JD012876

increased wave-mean flow interactions in the stratosphere can affect tropospheric variability reflected as changes in the annular modes [*Hartmann et al.*, 2000]. Previous work on the relationship between the annular modes and the BDC has focused on their interannual variations. For example, *Limpasuvan and Hartmann* [2000] and *Hartmann et al.* [2000] found that a high index of the northern annular mode (NAM) is associated with a poleward shift of the tropospheric jet and a stronger polar vortex, which decreases the refractive index and leads to a reduction of the stratospheric wave drag and a weaker BDC. But this relationship does not appear to apply to the trends of the NAM and the stratospheric wave drag [*Hu and Tung*, 2002]. In the Southern Hemisphere (SH), *Fogt et al.* [2009] found that the spring stratospheric wave driving is significantly correlated with the summer southern annular mode (SAM), suggesting a close relationship between the BDC and SAM on the intra-annual and interannual time scale.

[5] At present, the relationship between the trends in the annular modes and the strength of the BDC is poorly understood. The motivation of this paper is the similar seasonality of the trends in the SAM and the BDC in the late twentieth century, which suggests that the long-term trends in the SAM and the BDC could be closely related. The SAM is the dominant pattern of variability in the SH troposphere, which describes the fluctuations in geopotential height, temperature, zonal wind, and surface pressure with opposite signs in high and middle southern latitudes [*Thompson and Wallace*, 2000]. Observational studies have identified a significant trend of the SAM toward its positive phase (or a high index) during the late twentieth century, characterized by a strengthening of the Antarctic polar vortex and a poleward shift of the tropospheric jet with the largest seasonal trend occurring in the austral summer [*Thompson and Solomon*, 2002; *Marshall*, 2003]. Similar seasonality in the trend of the BDC has been reported in a number of coupled chemistry-climate model (CCM) investigations [*Butchart et al.*, 2006; *Li et al.*, 2008]. *Li et al.* [2008] further showed that this seasonal structure in the BDC trend is mainly caused by large increases in the SH downwelling during the austral summer. In addition, previous studies have found that Antarctic ozone depletion has a significant impact on the seasonality of the trends in the SAM [*Cai and Cowan*, 2007; *Perlwitz et al.*, 2008] and the BDC [*Li et al.*, 2008; *McLandress and Shepherd*, 2009; *Oman et al.*, 2009].

[6] The purpose of this paper is to investigate whether and how trends in the SAM and the BDC are related in the austral summer by examining simulations from the Goddard Earth Observing System (GEOS) CCM. We focus on the BDC-SAM relationship over the decadal time scale, but we also address their link on the interannual time scale. The model and simulations used in this paper are described in section 2. Results are presented in section 3. Conclusions and discussions are given in section 4.

2. Model and Simulations

[7] This study uses simulations with version 1 of the GEOSCCM. Details of the model can be found in the work of *Pawson et al.* [2008]. The model is an extension of the GEOS-4 General Circulation Model with a comprehensive stratospheric chemistry module. It uses a flux form semi-Lagrangian dynamical core, and the physics are adapted from the National Center for Atmospheric Research (NCAR) CCM3. The stratospheric chemistry module is from the Goddard Chemical Transport Model [*Douglass et al.*, 1996]. The model chemistry is coupled with physical processes through the radiation code. The model has 55 vertical levels with a top at 0.01 hPa. Simulations used in this study were performed with a horizontal resolution of 2° latitude by 2.5° longitude.

[8] For this study, we present results from three simulations of the latter half of the twentieth century (1960–2000). The first two experiments P1 and P2 are a two-member ensemble simulation (with different initial conditions) forced with observed, time-dependent sea surface temperature and sea ice amounts from HadISST and the CCMVal REF1 scenario of GHGs and ozone-depleting substances (ODSs) [*Eyring et al.*, 2005]. The mean of P1 and P2 in this study is denoted as P12. The third run Cl60 is identical to the first two except that the halogen concentrations are fixed at 1960 levels. The purpose of Cl60 is to separate the impacts of GHG and ODS.

[9] *Eyring et al.* [2006] evaluated simulations of temperature, trace species, and ozone for the period 1980–1999 from P1 and 12 other CCMs. *Pawson et al.* [2008] assessed ozone-temperature coupling in P1 and P2. Overall P1 and P2 results agree well with observations in terms of the stratospheric thermal structure and trace gas distributions. Long-term stratospheric temperature trend and ozone depletion in P1 and P2 are in reasonable agreement with observations. As with other CCMs, GEOSCCM has biases. One that is relevant to this study is that the Antarctic vortex is too persistent [*Pawson et al.*, 2008; *Hurwitz et al.*, 2010]. This will be discussed in section 4.

3. Model Results

[10] A key factor to understand the relationship between the trends in the BDC and SAM is their seasonality. This is illustrated by comparing the seasonal structure of trends in the net SH downward mass flux and the Antarctic geopotential height in the P12 simulations, which represent the seasonality of trends in the BDC and the SAM, respectively (Figure 1). Here and for the rest of this study, the trend is calculated by a linear least squares regression. The statistic significance of the trend is calculated using a two-tailed Student's t test with the degrees of freedom reduced from a lag-1 autocorrelation of regression residuals [*Santer et al.*, 2000]. The net hemispheric downward mass flux has been widely used as a measure of the strength of the BDC and is calculated by

$$2\pi \int_{\varphi_t}^{\text{pole}} a\rho \cos\varphi \overline{w^*} a d\varphi,$$

where $\overline{w^*}$ is the residual vertical velocity, ρ is the density, a is the Earth's radius, and φ_t is the southern turnaround latitude where the tropical upwelling changes to extratropical downwelling [*Butchart et al.*, 2006]. The SAM characterizes the seesaw pattern of geopotential height changes between Antarctica and the middle latitudes, and thus the seasonal structure of the trend in the Antarctic geopotential height can illustrate the seasonality of the trend in the SAM

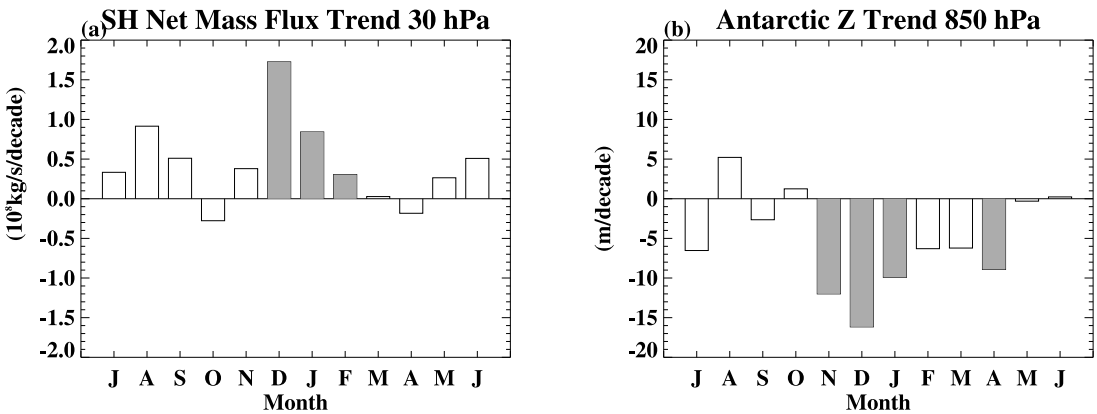

Figure 1. Seasonal cycle of linear trends in the period 1960–2000 for (a) 30 hPa net SH downward mass flux and (b) 850 hPa Antarctic (65°S–90°S) geopotential height in the P12 simulations. Shading indicates that trends are statistically significant at the 95% confidence level.

[*Thompson and Solomon*, 2002]. Figure 1 shows that the net SH downward mass flux at 30 hPa (Figure 1a) and the Antarctic geopotential height at 850 hPa (Figure 1b) have the largest and statistically significant (95% confidence level) trends in the austral late spring and summer (November–February). The increase in the net SH downwelling indicates an acceleration of the southern BDC, whereas the falling of the geopotential height indicates a trend of the SAM toward its positive phase. If we calculate the trends for the seasonal mean net downward mass flux, then both the summer (December–February) and winter (June–August) trends are statistically significant, but the summer trend is about one-third larger than the winter trend. Similar seasonal structure in the net SH downward mass flux is found in other lower stratosphere levels. For the geopotential height change over the Antarctic troposphere, Figure 1b shows a smaller but statistically significant decreasing trend in April. This seasonal structure in the P12 simulations agrees well with *Thompson and Solomon* [2002], who identified substantial decreasing trend in the tropospheric geopotential height over Antarctica in the austral summer and fall using radiosonde data.

[11] Figure 2a shows the seasonal evolution of the Antarctic geopotential height trend for the period 1960–2000. In the stratosphere, the geopotential height within the polar cap decreases from October to May with the largest drop in late spring and early summer (statistically significant at the 95% confidence level). This large decrease in the stratospheric geopotential height from November to February is caused by a strong cooling in the Antarctic lower stratosphere that peaks in November and extends to February (Figure 2b, recall that, assuming constant surface pressure, geopotential height represents the vertical integral of temperature $Z(p) = -\int_{\text{psurf}}^{p} \frac{RT(p)}{g} d\ln p$). During November–January, the geopotential height decrease extends from the stratosphere to the surface (Figure 2a). These features agree very

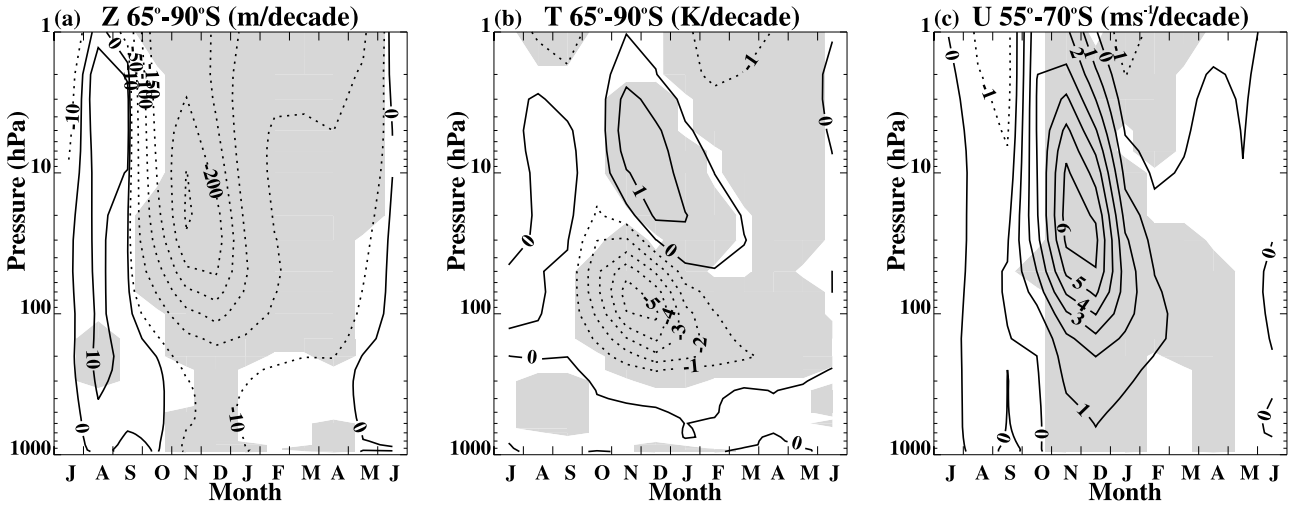

Figure 2. Linear trends plotted as function of month and pressure in (a) Antarctic geopotential height (65°S–90°S), (b) Antarctic temperature (65°S–90°S), and (c) circumpolar zonal wind (55°S–70°S) in the P12 simulations. Shading indicates that trends are statistically significant at the 95% confidence level.

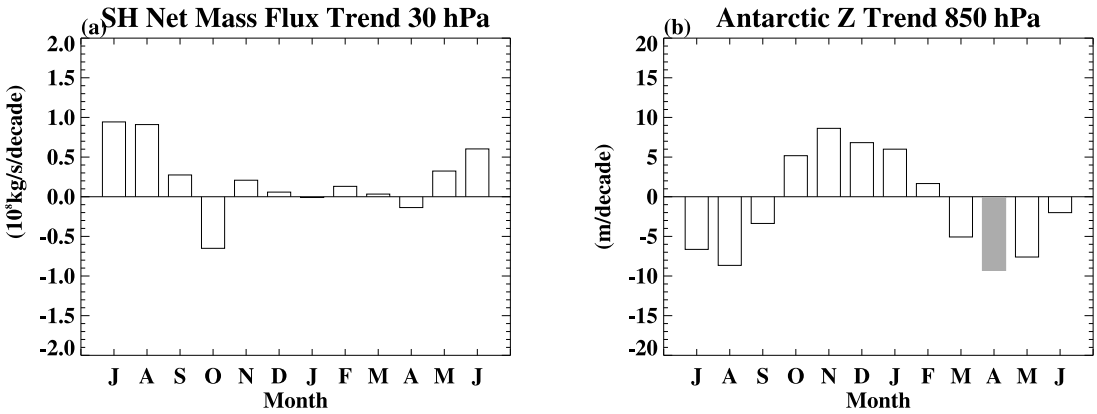

Figure 3. Same as Figure 1 but for the Cl60 simulation.

well with observations [*Thompson and Solomon*, 2002]. The cooling in the Antarctic lower stratosphere also produces a large westerly shift of the circumpolar flow in the stratosphere that is coupled with an enhanced westerly flow throughout the troposphere from November to January (Figure 2c).

[12] Several observational [*Thompson and Solomon*, 2002] and modeling studies [*Cai and Cowan*, 2007; *Perlwitz et al.*, 2008] have suggested that the large summer SAM trend is related to Antarctic ozone depletion. Strengthening of the BDC during the austral summer in the recent past has also been largely attributed to Antarctic ozone depletion [*Manzini et al.*, 2003; *Li et al.*, 2008; *McLandress and Shepherd*, 2009]. In our simulations, the role of Antarctic ozone depletion in driving trends in the BDC and the SAM can be clarified by comparing the P12 and Cl60 results. Again, Cl60 is same as P12 except that the halogen loading is fixed at 1960 levels and, therefore, has no Antarctic ozone hole. Without ozone depletion, there is no significant trend in the 30 hPa net SH downward mass flux in December–February (Figure 3a) when the P12 simulations show the largest increase (see Figure 1a for comparison). The trend in the Antarctic geopotential height at 850 hPa in Cl60 (Figure 3b) also has totally different seasonal structures from that in P12 (see Figure 1b). The lower tropospheric geopotential height over Antarctica actually increases (although not statistically significant) in late spring and early summer in Cl60 (also see Figure 4a) due to GHG increase-induced tropospheric warming (Figure 4b). Comparing temperature changes in the Antarctic stratosphere between Cl60 and P12 reveals that the strong lower stratospheric cooling and the significant middle stratospheric warming are driven by the ozone hole (Figures 4b and 2b). Figure 4c shows that in Cl60 the circumpolar flow does not have a significant trend from November to February in the troposphere and stratosphere, in contrast to the strong westerly accelerations in the P12 simulations. These different changes between the P12 and Cl60 simulations clearly show that the large summer SAM and BDC trends are driven by Antarctic ozone depletion.

[13] The connection between Antarctic ozone depletion and the strengthening of the BDC in the SH is well understood [e.g., *Li et al.*, 2008]. Ozone hole cools the Antarctic lower stratosphere, increases the meridional temperature gradient in the subpolar region, and strengthens the westerly

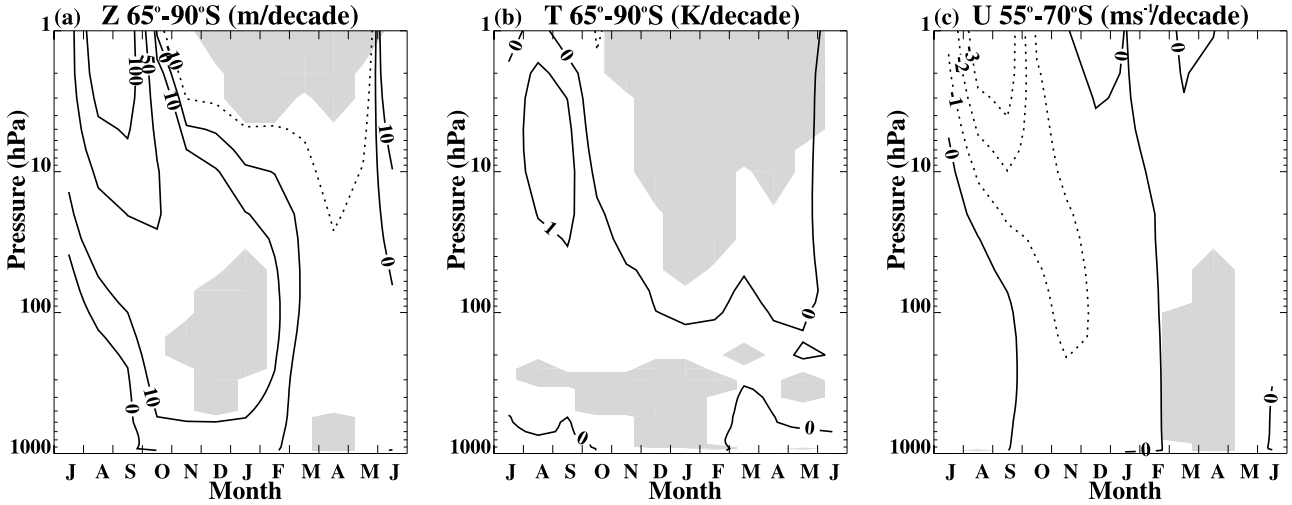

Figure 4. Same as Figure 2 but for the Cl60 simulation.

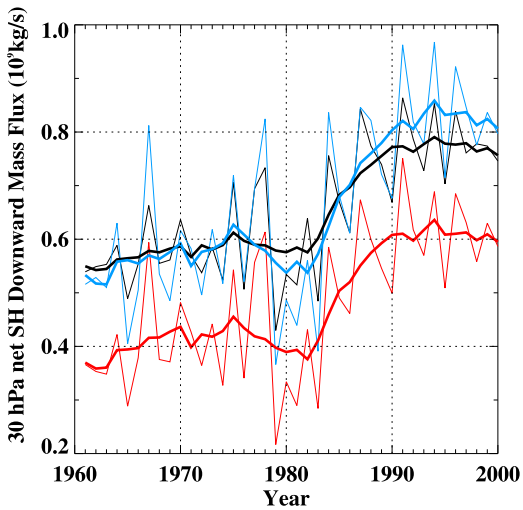

Figure 5. Time series of the NDJF mean net SH downward mass flux at 30 hPa (black). The red and blue lines are the wave-driven mass fluxes calculated from the downward control principle. The red lines show the results from model resolved waves (EP flux divergence) only. The blue lines show the results including both resolved waves and parameterized gravity waves. The thick curves are 7 year running average mean.

circumpolar flow. As a result, the breakup of the Antarctic polar vortex is delayed from late spring to early summer. A direct consequence of the delayed polar vortex breakup is that the stratospheric planetary wave activity emanating from the troposphere can penetrate higher and stay longer in the stratosphere, causing an acceleration of the BDC. It should be noted that an underlying assumption of the above argument is that the strengthening of the southern BDC can be accounted for by increases in the planetary wave forcing. Therefore, we first need to verify whether this is indeed the case in the P12 simulations in order to apply the delayed polar vortex breakup mechanism to explain the seasonality of the BDC trend.

[14] Figure 5 compares the evolution of the November–February (NDJF) 30 hPa net SH downward mass flux and the contributions from model resolved waves and parameterized gravity waves calculated from the downward control principle [*Haynes et al.*, 1991]. We choose NDJF because the net SH stratospheric mass flux increase and the lower tropospheric Antarctic geopotential height drop are largest during this 4 month period (see Figure 1). Figure 5 shows that the actual net SH mass flux agrees very well with the wave-driven mass flux from the downward control analysis. Model-resolved waves and parameterized gravity waves account for 72% and 28%, respectively, of the net SH downward mass flux at 30 hPa, consistent with previous studies [e.g., *Butchart et al.*, 2006]. The long-term and interannual variations of the mass flux driven by EP flux divergence are in very good agreement with the actual mass flux with a correlation of 0.97. We conclude that the strengthening of the SH extratropical BDC is mostly due to the increase in the stratospheric planetary wave forcing.

[15] Figure 5 also shows that the change of the net SH downwelling during NDJF is not a linear trend. There is an abrupt increase around 1980 and the trend for the period 1981–2000 is much larger than that for the period 1960–1980. We found that the NDJF net SH downwelling is highly correlated with the October Antarctic total ozone (r = 0.90) (Figure 6), which suggests that the strength of the southern summer BDC is strongly affected by the severity of Antarctic ozone depletion. Similar temporal structures are also found in the evolution of the Antarctic geopotential height during NDJF in both the troposphere and the stratosphere (Figure 6). The time series of the 30 and 850 hPa geopotential height are highly correlated with each other (r = 0.78), and they are both strongly correlated with the October Antarctic total ozone (r = 0.89 and 0.59, respectively) and the 30 hPa net SH downward mass flux (r = 0.78 and 0.62, respectively). *Thompson and Solomon* [2002] identified strong correlations between Antarctic ozone depletion and the falling of the tropospheric and stratospheric geopotential height in the southern high latitudes using observational data and argued that these correlations suggest a significant impact of the ozone hole on the SAM trend. Our P12 results support their argument and also reveal a possible linkage between the BDC and SAM through their close connection with the Antarctic ozone hole.

[16] The relationship between the changes in the southern extratropical BDC and SAM in the P12 simulations is investigated by comparing the trend of the residual circulation with the regression (or covariance) of the residual circulation on the SAM index. We follow the method of *Thompson et al.* [2000] to define the SAM as the first

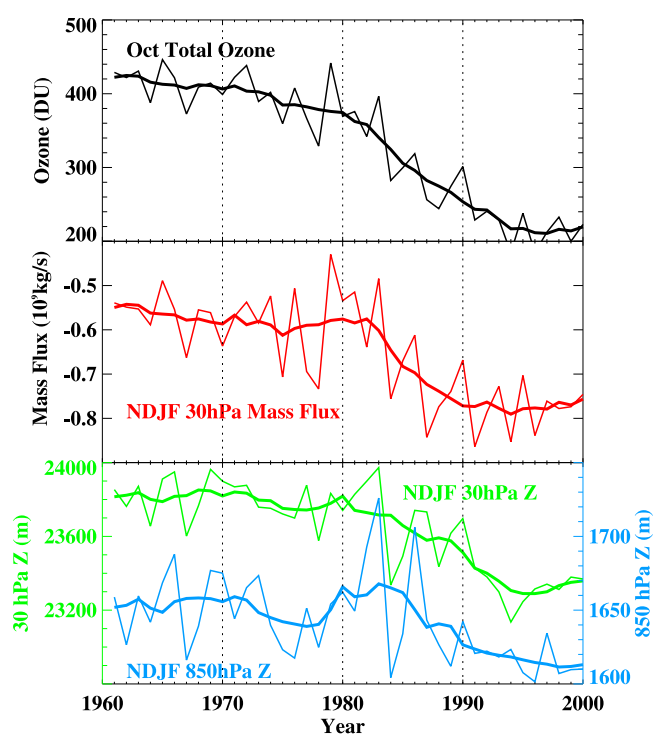

Figure 6. Time series of (top) October Antarctic total ozone, (middle) the negative of the NDJF mean net SH mass flux at 30 hPa, and (bottom) NDJF mean geopotential height at 30 hPa (green, left axis) and 850 hPa (blue, right axis). Thick curves are 7 year running average mean.

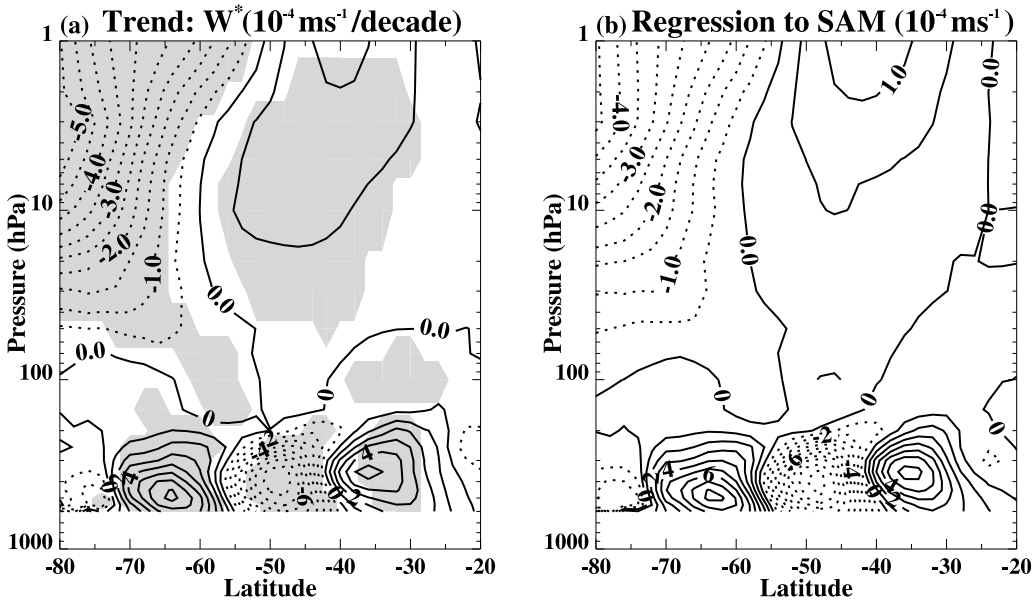

Figure 7. (a) Linear trends of the NDJF residual vertical velocity in the period 1981–2000 as a function of latitude and pressure. Shading denotes that trends are significantly different from zero at the 95% confidence level. (b) NDJF residual vertical velocity regressed on the standardized SAM index.

empirical orthogonal function (EOF) of the 850 hPa geopotential height southward of 20°S. The EOFs are calculated using NDJF mean time series for the period 1981–2000, and the standardized leading principal component time series is used as the SAM index. The calculated SAM index using this method is very similar to the inverted 850 hPa Antarctic geopotential height (see Figure 6). Results presented in the following are not sensitive to the definition of the SAM pattern and index. For example, we can use the circumpolar upper tropospheric zonal wind as the SAM index and obtain the same results. We focus on the 20 year period 1981–2000, because changes in the BDC and SAM are much larger than those in the period 1960–1980 (Figure 6).

[17] The linear trend of the residual vertical velocity in NDJF between 1981 and 2000 in P12 is shown in Figure 7a as a function of latitude and pressure. In the stratosphere, the trend in the residual vertical velocity demonstrates an accelerated BDC with enhanced downwelling in the southern high latitudes (dashed contours) and increased upwelling in the midlatitudes (solid contours). Very similar spatial patterns are found in the SAM regression map (Figure 7b), showing that an anomalously strong BDC is associated with a high index of the SAM. The nearly identical patterns in Figures 7a and 7b illustrate that the long-term change of the strengthening of the BDC is highly projected onto the trend of SAM toward its high index. The trend in the residual vertical velocity that is linearly congruent with the SAM index, obtained by multiplying the covariance with the linear trend of the SAM index, can be used to quantify the relationship between trends in BDC and SAM [*Thompson and Solomon*, 2002]. The SAM index has a linear trend of 0.90/decade for the period 1981–2000 in the P12 simulations; thus, it can be inferred that more than 80% of increases in the Antarctic downwelling and midlatitude upwelling are linearly congruent to the SAM index. Furthermore, almost all the tropospheric trend in the residual vertical velocity is linearly projected onto the SAM.

[18] Although the BDC does not show a significant linear trend in NDJF in Cl60 (Figure 3a), it is still worthy to examine whether the interannual variations of the BDC are related to those of SAM in Cl60. Figure 8a shows that the linear trend in the stratospheric residual vertical velocity is not statistically significant and does not resemble the SAM regression map. However, the SAM index regression map in Cl60 (Figure 8b) has a nearly identical pattern to that for P12 (Figure 7b). The magnitude of the regression coefficients is smaller in Cl60 than in P12, because the trends of the BDC and SAM in P12 yield larger covariance. When the covariance between the residual vertical velocity and the SAM in P12 is calculated using detrended data, the resulting regression coefficients have nearly the same magnitude as those in Cl60 (figure not shown). The similar regression patterns in P12 and Cl60 illustrate that, regardless of ozone depletion, a high SAM index is associated with anomalously strong polar downwelling and midlatitude upwelling in austral summer on the interannual time scale. The impact of the Antarctic ozone hole is to drive a long-term trend in the BDC that is strongly congruent with the year-to-year SAM variations.

[19] In order to understand why trends in the southern BDC are strongly reflected in the SAM index in the P12 simulations, we need to find out the cause for the acceleration of the BDC and its connection with the SAM. We have already shown in Figure 5 that the strengthening of the BDC in the austral summer is mostly due to increase in the stratospheric planetary wave driving. Thus, the question is how the enhanced planetary wave driving is related to the SAM. In order to answer this question, we examine the linear trends in the NDJF zonal mean temperature, zonal wind, eddy momentum, and heat flux between 1981 and

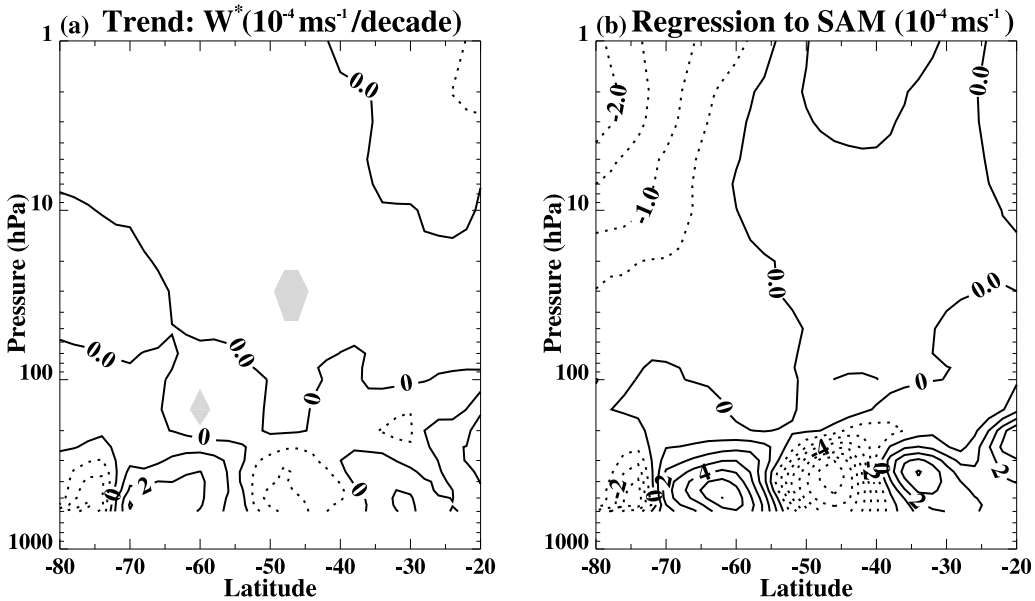

Figure 8. Same as Figure 7 but for the Cl60 simulation.

2000 and their SAM regression maps (Figure 9). Temperature changes in the summer Antarctic stratosphere are marked by a vertical dipole structure (Figure 9a) that has been reported in many model simulations [e.g., *Mahlman et al.*, 1994] and has been confirmed in radiosonde and reanalysis data [*Randel and Wu*, 1999]. The strong Antarctic lower stratospheric cooling increases the meridional temperature gradient and enhances the stratospheric westerlies over the high latitudes (Figure 9b). In NDJF, a westerly shift of the SH stratospheric flow indicates a delay of the polar vortex breakup, which prolongs the period of weak westerlies in the lower stratosphere and increases the upward propagation of planetary wave activity into the stratosphere. This is illustrated in Figure 9c, showing a large increase in negative northward meridional eddy heat flux (an approximation of the vertical component of the EP flux) in the stratosphere poleward of about 50°S, which increases westward momentum deposition and strengthens the BDC. The westerly accelerations of the zonal wind in the SH high latitude stratosphere is coupled with increased westerlies in the troposphere centered at 60°S (Figure 9b). The tropospheric zonal wind trend is characterized by a dipole structure, indicating a poleward shift of the tropospheric jet. This poleward shift is maintained by a similar displacement of the eddy meridional flux of zonal momentum in the upper troposphere (Figure 9d).

[20] The SAM regression maps of the temperature, zonal wind, and eddy heat and momentum flux are presented in Figures 9e–9h. Nearly identical patterns are found between the regression maps and the linear trends, indicating that trends in the tropospheric and stratospheric circulations and wave activities are strongly projected onto the positive phase of the SAM. Multiplying the regression maps with the linear trend in the SAM index and comparing, we found that nearly all trends in the troposphere are congruent with the SAM index. More important for the purpose of this study, most of the stratospheric trends (about 80%) are congruent with the SAM index.

[21] Figures 10a–10d show that in the Cl60 simulation that does not include ozone depletion, linear trends of the NDJF zonal wind and eddy momentum and heat flux are not statistically significant. Although Cl60 simulates statistically significant temperature changes due to GHG increase, it does not reproduce the strong Antarctic lower stratospheric cooling and middle stratospheric warming. Comparing with the P12 results (Figures 9a–9d) clearly demonstrates that the trends in the P12 simulations are driven by the ozone hole. However, the SAM regression maps in Cl60 are very similar to those in P12, but with smaller covariance (Figures 10e–10h). When we remove the trends in the P12 results and calculate the regression, we find that the regression coefficients have nearly the same magnitude in P12 and Cl60. This similarity indicates that the relationship between interannual variations of the summer stratospheric circulation and SAM are robust, with or without ozone depletion.

[22] Our model-simulated austral summer circulation changes, and the SAM regression maps are in broad agreement with those calculated using the National Centers for Environmental Prediction (NCEP) Reanalysis 2 data. Figure 11 shows that the major features of the SH summer climate change agree qualitatively very well between the NCEP Reanalysis and the P12 runs, including the Antarctic lower stratospheric cooling, the strengthened circumpolar flow, and the enhanced stratospheric wave flux. There are no direct observations of the BDC (or the residual vertical velocity), but the increases of eddy heat flux in the mid-latitude to high latitude stratosphere in the NCEP Reanalysis (Figure 11c) support the modeled strengthening of the BDC. Figure 11 also shows that the trends resemble the regressions onto the SAM index, supportive of the BDC-SAM relationship in our model simulations. However, GEOSCCM overpredicts the trends and the covar-

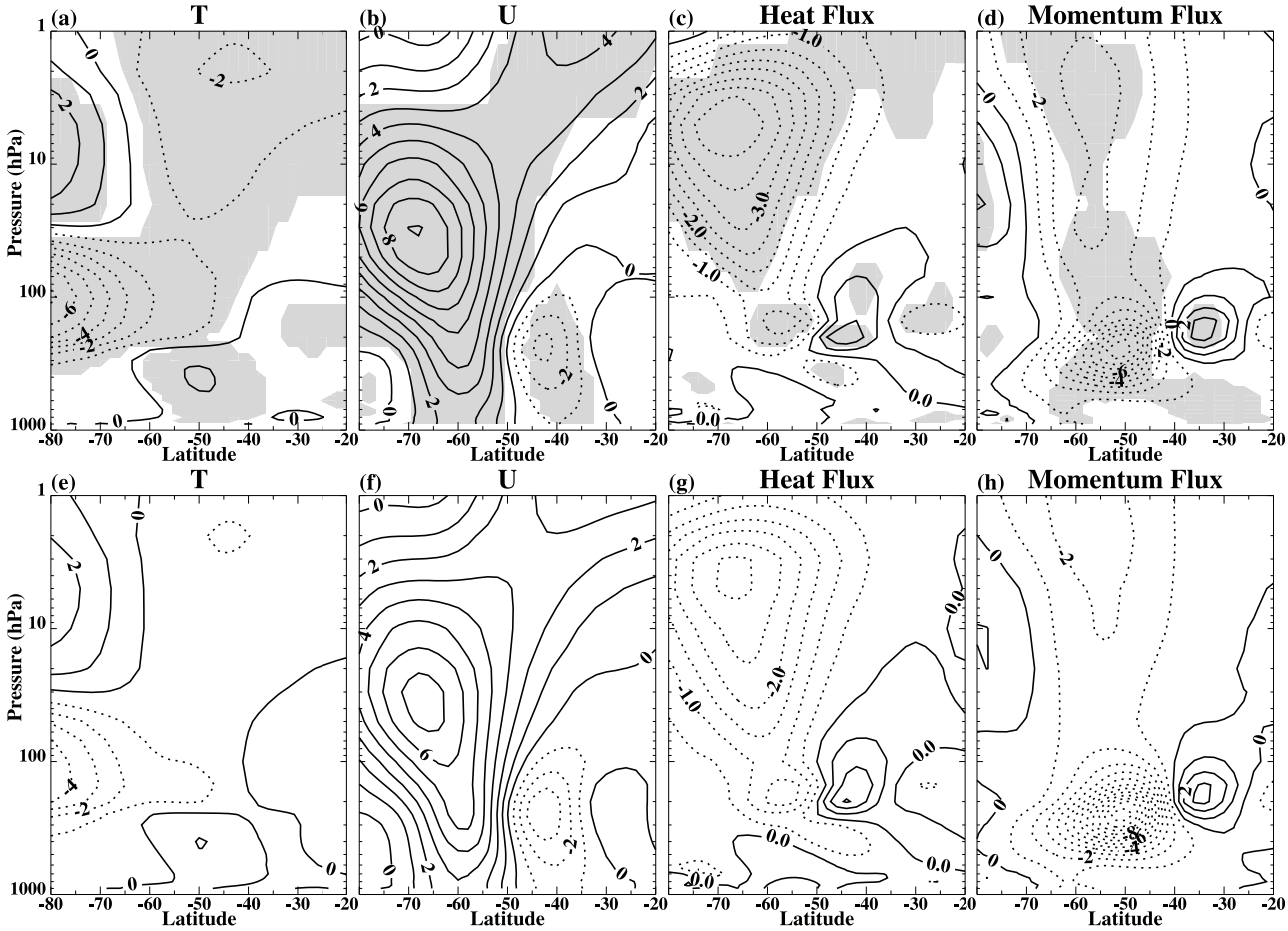

Figure 9. (top) Linear trends for the period 1981–2000 as a function of latitude and pressure for the NDJF mean (a) temperature (K/decade), (b) zonal wind (m s^{-1}/decade), (c) northward meridional eddy heat flux (k m s^{-1}/decade), and (d) meridional eddy flux of zonal momentum (m^2 s^{-2}/decade) in the P12 simulations. Shading denotes the 95% confidence level. (bottom) SAM regression maps for the NDJF mean (e) temperature (K/std SAM), (f) zonal wind (m s^{-1}/std SAM), (g) eddy heat flux (km s^{-1}/std SAM), and (h) eddy momentum flux (m^2 s^{-2}/std SAM).

iances with the SAM index. In section 4, we discuss why the BDC-SAM relationship is amplified in the simulations.

[23] The above analyses suggest that the key to understanding the BDC-SAM relationship in the austral summer is to link the circumpolar westerly anomalies and enhanced wave activity in the stratosphere to a high index of the tropospheric SAM. There is growing observational evidence that such stratospheric anomalies induce tropospheric variability reflected as a positive phase of the annular modes [e.g., *Baldwin et al.*, 2003; *Thompson et al.*, 2005; *Fogt et al.*, 2009]. Here we suggest a possible mechanism to explain the link between the ozone hole, the strengthening of the BDC, and the SAM trend: the ozone hole increases the stratospheric wave driving and strengthens the BDC through a delayed vortex breakup, which in turn forces a SAM trend toward its high index. One way to test this hypothesis is to remove the SAM variability that is linearly congruent with the stratospheric wave driving and check the relationship between the SAM residual and the stratospheric ozone concentration. If the SAM residual is correlated with the stratospheric ozone and has a significant trend, this would suggest that other processes in addition to stratospheric wave driving are involved in linking the ozone hole with the tropospheric SAM trend. We found that, after removing the part of SAM index that is congruent with the NDJF 30 hPa mass flux, the SAM index residual does not have a statistically significant trend and is not significantly correlated with the October total column ozone ($r = -0.14$ after removal of trends) for the 1960–2000 period in the P12 runs (similar results are obtained for the period 1981–2000 with $r = -0.20$). In comparison, as can be inferred from Figure 6, the NDJF SAM index is highly correlated with October total ozone ($r = -0.52$ after removal of trends) and has a statistically significant trend. These results appear to support our hypothesis that Antarctic ozone depletion forces a summer tropospheric SAM trend almost entirely through changes in stratospheric wave driving. However, it should be noted that the above analysis does not rule out other mechanisms for stratospheric anomalies to affect the SAM. For example, the SAM trend could be driven by the circumpolar westerly anomalies in the upper troposphere and lower stratosphere through the mechanism

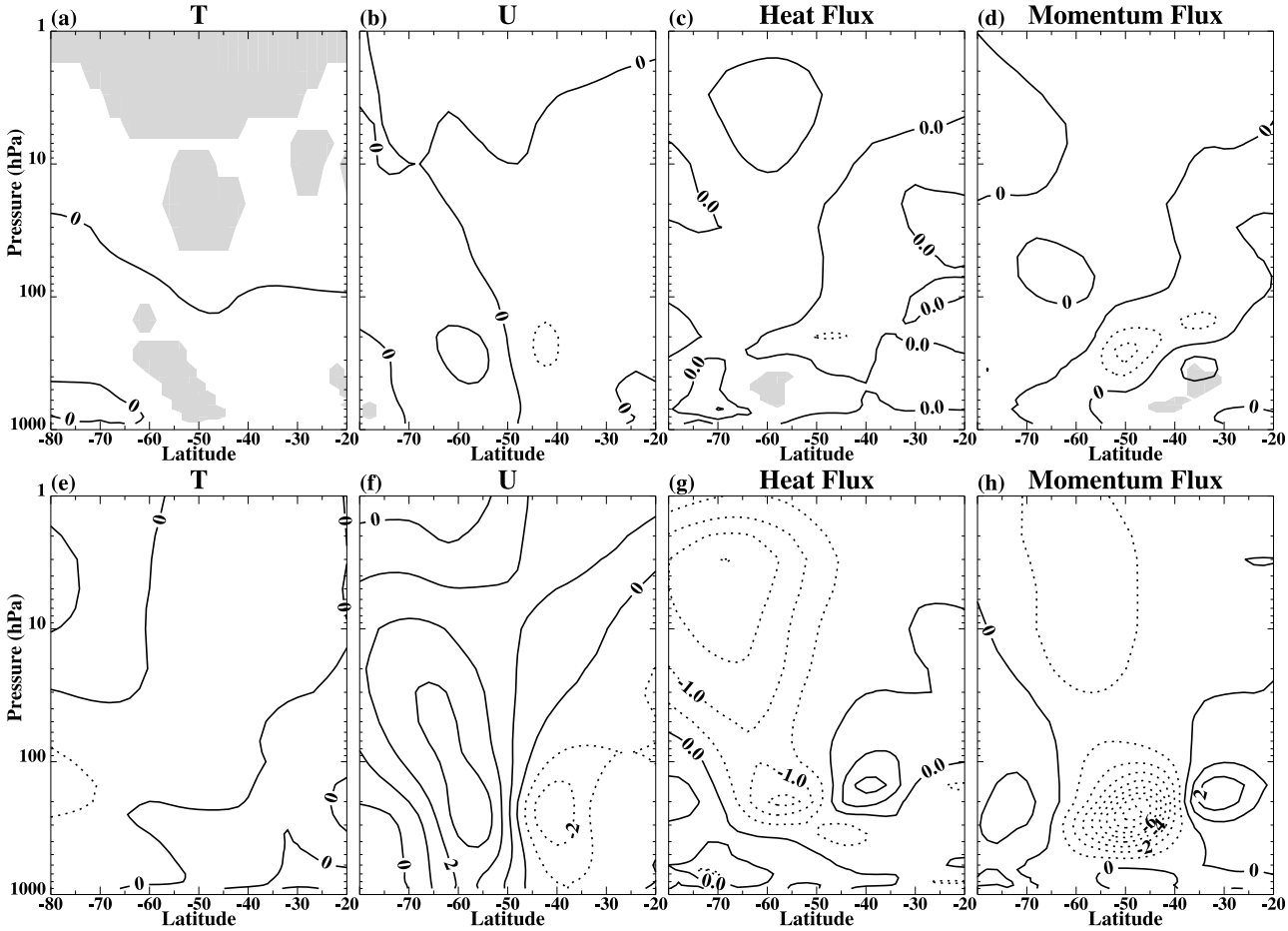

Figure 10. Same as Figure 9 but for the Cl60 simulation.

suggested by *Chen and Held* [2007]. Therefore, it is possible that the increased and extended westerlies themselves could be responsible for the BDC-SAM connection.

4. Discussion and Conclusions

[24] The relationship between the BDC and the SAM in the austral summer is investigated with GEOSCCM simulations. In the P12 integrations, which simulates the observed depletion of ozone, the southern BDC accelerates and the SAM shifts toward a higher index during NDJF in the latter half of the twentieth century. The two trends overlap: the strengthening of the BDC is strongly projected onto the high index of the SAM, and vice versa. In contrast, in Cl60, which does not simulate ozone depletion, neither the SAM nor the BDC has a significant trend during NDJF. These model results clearly demonstrate that Antarctic ozone depletion drives changes in the BDC and the SAM. We suggest that the ozone hole-induced delay of the Antarctic vortex breakup is the key to linking the strengthening of the BDC with the SAM during the austral summer. The delayed onset of easterlies in the Antarctic lower stratosphere prolongs the period for dynamical stratosphere-troposphere interactions. A direct consequence of the persistent stratospheric westerlies is to strengthen the summer BDC by allowing more tropospheric planetary wave activity entering the stratosphere, as shown in Figures 9 and 11. On the other hand, the enhanced stratospheric wave driving or the increased westerlies forces a SAM trend toward its high index. In summary, the BDC-SAM relationship is a result of increased stratosphere-troposphere coupling driven by ozone depletion.

[25] Although the Cl60 simulation does not produce statistically significant trends in the BDC and the SAM during NDJF, it reproduces the same interannual relationship between the BDC and the SAM as that in the P12 simulations. This result raises a question: Is the physical mechanism that links the trends in the BDC and the SAM the same as the mechanism that operates on the interannual time scale? In order to answer this question, first we need to find out what drives the interannual relationship between the summer SAM and the BDC. *Fogt et al.* [2009] investigated intra-annual relationships between the Antarctic total column ozone, the SAM, and the stratospheric wave activity in the latter half of the twentieth century using observations and the same GEOSCCM simulations analyzed in this study. They found that, in addition to the well-known negative correlation between the spring Antarctic ozone and the summer SAM, the spring stratospheric wave driving also plays an important role in determining the interannual variability of the summer SAM. The results of *Fogt et al.* [2009] suggest, based on the positive correlation

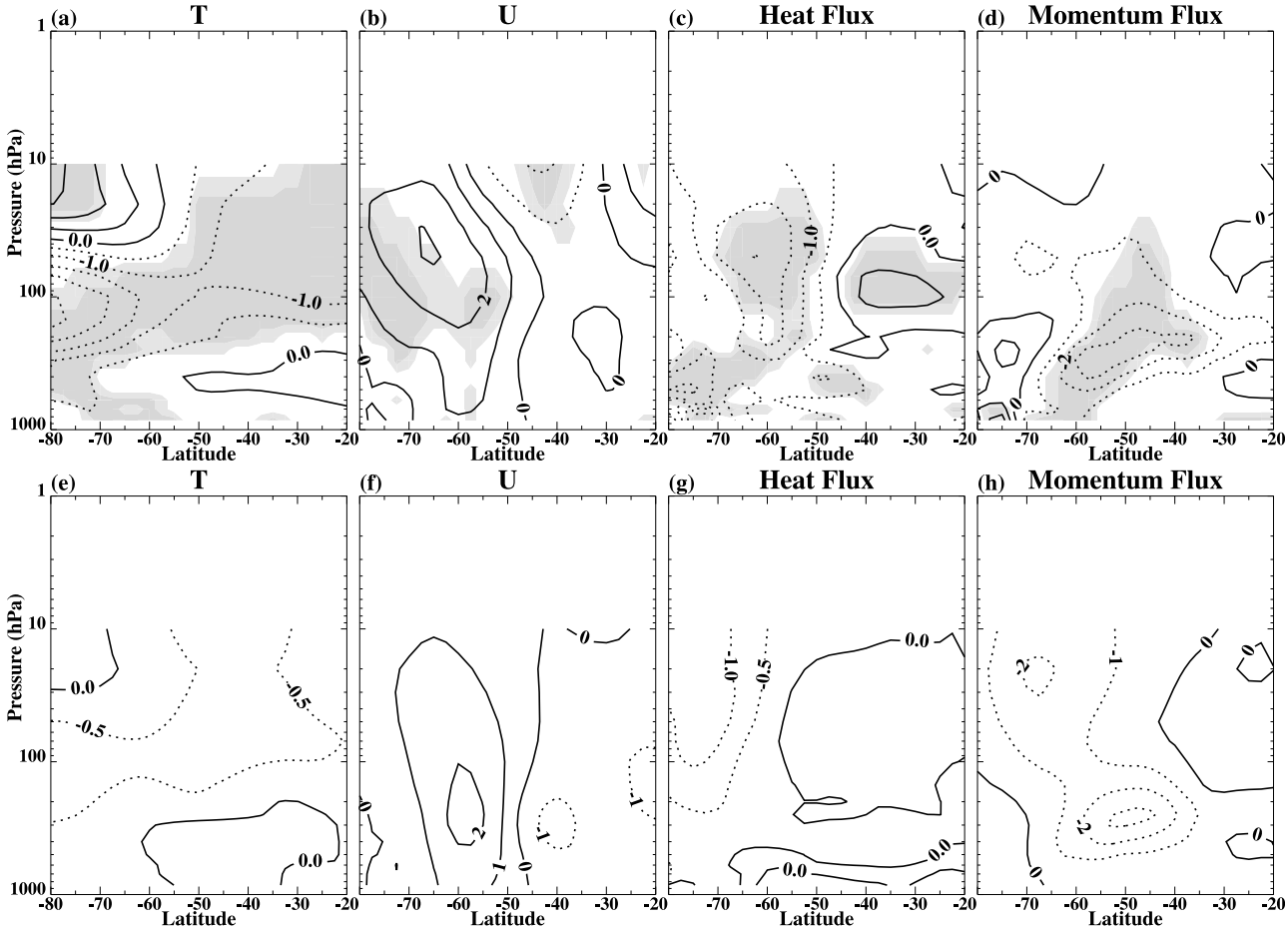

Figure 11. Same as Figure 9 but calculated from the NCEP Reanalysis 2 data. The dark and light shadings denote 95% and 90% confidence levels, respectively. Note that the NCEP data are only available below 10 hPa.

between the summer SAM and BDC identified in this study, that the stratospheric wave activity (or BDC) in spring could significantly affect the wave activity in summer and is important in driving the interannual BDC-SAM relationship. This is confirmed by the high negative correlation between the early spring BDC and the summer SAM ($r = -0.56$ between October 30 hPa SH mass flux and the NDJF SAM index), and between the early spring BDC and late spring/early summer BDC ($r = -0.55$ between October and December/January 30 hPa mss flux) in the P12 simulations (correlation is calculated after removal of linear trends).

[26] We suggest that the mechanism by which the spring stratospheric wave activity affects the interannual variability of the summer BDC and SAM is the same as that explaining how ozone depletion drives the decadal variations of the summer BDC and SAM, i.e., through its impact on the persistence of the Antarctic vortex leading to changes in stratosphere-troposphere coupling. *Hurwitz et al.* [2010] showed that the Antarctic polar vortex breakup date is highly correlated with the spring stratospheric wave driving in the NCEP and ERA40 reanalysis data and in the simulations with a newer version of GEOSCCM. This relationship results from a 1 month lag correlation between the midlatitude wave driving and the polar stratospheric temperature [e.g., *Austin et al.*, 2003]. Anomalously weak eddy heat flux in early-middle spring leads to an anomalously cold polar stratosphere in late spring and a delayed vortex breakup, which extends the period of active stratosphere-troposphere dynamical coupling and causes a stronger summer BDC and SAM. However, it should be emphasized that the decadal trends of the summer BDC and SAM cannot be attributed to long-term changes in spring stratospheric wave driving. In the P12 simulations, the BDC in October does not have a statistically significant trend (Figure 1a). *Waugh et al.* [1999] found that in the NCEP Reanalysis data, the SH eddy heat flux at 100 hPa in early spring increases from 1979 to 1998, which cannot explain the prolonged persistence of the Antarctic vortex during this period.

[27] It is interesting to compare the interannual BDC-SAM relationship identified in this paper to the BDC-NAM relationship reported in previous studies. *Limpasuvan and Hartmann* [2000] and *Hartmann et al.* [2000] found that a higher NAM index is associated with a weaker stratospheric wave driving and hence a weaker BDC in the Northern Hemisphere (NH) high latitudes during the NH winter. This is opposite to the positive correlation between the BDC and SAM during the austral summer. The different relationships between the BDC and the annular modes in the NH

and SH are due to the different seasonality of the SAM and NAM. The NAM is actively coupled with the stratospheric circulation in winter, whereas the SAM's active season is in late spring [*Thompson and Wallace*, 2000]. In the NH winter, a high NAM index is associated with a stronger Arctic vortex and stronger circumpolar westerlies, which decrease the refractive index and reduce wave activity entering polar stratosphere [*Limpasuvan and Hartmann*, 2000; *Hu and Tung*, 2002]. But in the SH summer a high SAM index is associated with a colder Antarctic lower stratosphere, which delays the breakdown of the Antarctic vortex and strengthens the BDC. From the above argument, one expects that the BDC-SAM relationship would reverse during the austral winter, and this is confirmed in the GEOSCCM simulations (figure not shown).

[28] There are no direct observations of the BDC, and hence, the modeled BDC-SAM relationship could not be directly verified. *Stolarski et al.* [2006] found indirect evidence of a strengthened BDC from the observed ozone increase just above the ozone hole in the austral summer in satellite measurements, which supports our findings. More importantly, the key to understanding the BDC-SAM relationship is reasonably represented in the model simulations compared with the NCEP Reanalysis data. As has shown in Figure 11, the ozone hole-induced delay of the Antarctic vortex breakup and the stratospheric wave flux increases in our simulations agree qualitatively very well with the reanalysis data. However, it is also apparent that the model overpredicts the BDC-SAM relationship and the austral summer climate change.

[29] As briefly mentioned in section 2, GEOSCCM has a "cold pole" bias in the spring Antarctic stratosphere, a common problem in middle atmosphere models [*Eyring et al.*, 2006]. Because of the cold bias, the modeled Antarctic vortex is too persistent and breaks up about 2 weeks later than observed [*Hurwitz et al.*, 2010]. *Fogt et al.* [2009] found that, as a consequence of the later than observed Antarctic vortex breakup, GEOSCCM amplifies troposphere-stratosphere coupling and SAM persistence and hence overpredicts the spring ozone-summer SAM relationship. These model deficiencies have important implications for the simulated BDC-SAM relationship reported in this study, because this relationship is driven by stratosphere-troposphere coupling. Therefore, while the simulated BDC-SAM relationship qualitatively agrees with the reanalysis data, this relationship is amplified in our model simulations. More generally, results presented here and those in the works of *Fogt et al.* [2009] and *Hurwitz et al.* [2010] indicate that a too persistent model Antarctic vortex leads to overpredictions of the impacts of the ozone hole on the austral summer climate change in the late twentieth century, which also implies that the model would unrealistically amplify the ozone recovery effects on climate change in the 21st century as well. Therefore, as pointed out by *Fogt et al.* [2009] and *Hurwitz et al.* [2010], improving the model presentation of the persistence of Antarctic vortex is critical to correctly predict the interactions between ozone depletion, ozone recovery, and climate change in the troposphere and stratosphere.

[30] Finally, the mechanism by which increased stratospheric wave activity and westerlies drive a SAM trend or more generally the mechanism for the stratospheric variability to affect the tropospheric circulation is not clear. Currently, there exist several hypotheses, including downward propagation of wind anomalies driven by eddy-mean flow interactions [*Christiansen*, 2001], amplification of tropospheric response to lower stratospheric wind anomalies [*Song and Robinson*, 2004], and increases of tropospheric eddy phase speed leading to a poleward displacement of the subtropical wave breaking zone [*Chen and Held*, 2007]. There is growing evidence that the stratosphere has impacts on the troposphere, and understanding its dynamical mechanism is certainly an important research issue.

[31] **Acknowledgments.** This work was supported by NASA's Modeling and Analysis program. We thank three anonymous reviewers for their insightful comments. The NCEP Reanalysis 2 data are provided by the NOAA/OAR/ESRL PSD, Boulder, CO, USA, from their Web site at http://www.esrl.noaa.gov/psd/.

References

Andrews, D. G., J. R. Holton, and C. B. Leovy (1987), *Middle Atmosphere Dynamics*, 485 pp., Academic, Orlando, Fla.

Austin, J., et al. (2003), Uncertainties and assessments of chemistry-climate models of the stratosphere, *Atmos. Chem. Phys.*, *3*, 1–27.

Baldwin, M. P., D. B. Stephenson, D. W. J. Thompson, T. J. Dunkerton, A. J. Charlton, and A. O'Neill (2003), Stratospheric memory and skill of extended-range weather forecasts, *Science*, *301*, 636–640.

Brewer, A. W. (1949), Evidence for a world circulation provided by the measurements of helium and water vapor distribution in the stratosphere, *Q. J. R. Meteorol. Soc.*, *75*, 351–363.

Butchart, N., and A. A. Scaife (2001), Removal of chlorofluorocarbons by increased mass exchange between the stratosphere and troposphere in a changing climate, *Nature*, *410*, 799–802.

Butchart, N., et al. (2006), Simulations of anthropogenic change in the strength of the Brewer-Dobson circulation, *Clim. Dyn.*, *27*, 727–741.

Cai, W., and T. Cowan (2007), Trends in the Southern Hemisphere circulation in IPCC AR4 models over 1950–99: ozone depletion versus greenhouse gas forcing, *J. Clim.*, *20*, 681–693.

Chen, G., and I. M. Held (2007), Phase speed spectra and the recent poleward shift of Southern Hemisphere surface westerlies, *Geophys. Res. Lett.*, *24*(21), L21805, doi:10.1029/2007GL031200.

Christiansen, B. (2001), Downward propagation of zonal mean wind anomalies from the stratosphere to the troposphere: Model and reanalysis, *J. Geophys. Res.*, *106*(D21), 27,307–27,322.

Dobson, G. M. B. (1956), Origin and distribution of the polyatomic molecules in the atmosphere, *Proc. R. Soc. London, Ser. A*, *236*, 187–193, doi:10.1098/rspa.1956.0127.

Douglass, A. R., C. J. Weaver, R. B. Rood, and L. Coy (1996), A three-dimensional simulation of the ozone annual cycle using winds from a data assimilation system, *J. Geophys. Res.*, *101*(D1), 1463–1474.

Eyring, V., et al. (2005), A strategy for process-oriented validation of coupled chemistry-climate models, *Bull. Am. Meteorol. Soc.*, *86*, 1117–1133.

Eyring, V., et al. (2006), Assessment of temperature, trace species, and ozone in chemistry-climate model simulations of the recent past, *J. Geophys. Res.*, *111*(D22), D22308, doi:10.1029/2006JD007327.

Fogt, R. L., J. Perlwitz, S. Paswson, and M. A. Olsen (2009), Intra-annual relationships between polar ozone and the SAM, *Geophys. Res. Lett.*, *36*(4), L04707, doi:10.1029/2008GL036627.

Garcia, R. R., and W. J. Randel (2008), Acceleration of the Brewer-Dobson circulation due to increases in greenhouse gases, *J. Atmos. Sci.*, *65*, 2731–2739.

Hartmann, D. L., J. M. Wallace, V. Limpasuvan, D. W. J. Thompson, and J. R. Holton (2000), Can ozone depletion and global warming interact to produce rapid climate change?, *Proc. Natl. Acad. Sci.*, *92*, 1412–1417.

Haynes, P. H., C. J. Marks, M. E. McIntyre, T. G. Shepherd, and K. P. Shine (1991), On the "downward control" of the extratropical diabitic circulation by eddy-induced mean zonal forces, *J. Atmos. Sci.*, *48*, 651–678.

Holton, J. R., P. H. Haynes, M. E. McIntyre, A. R. Douglass, R. B. Rood, and L. Pfister (1995), Stratosphere-troposphere exchange, *Rev. Geophys.*, *33*(4), 403–439.

Hu, Y., and K. K. Tung (2002), Interannual and decadal variations of planetary wave activity, stratospheric cooling, and Northern Hemisphere annular model, *J. Clim.*, *15* 1659–1673.

Hurwitz, M. M., P. A. Newman, F. Li, L. D. Oman, O. Morgenstern, P. Braesicke, and J. A. Pyle (2010), Assessment of the breakup of the

Antarctic polar vortex in chemistry-climate models, *J. Geophys. Res.*, *115*, D07105, doi:10.1029/2009JD012788.

Li, F., J. Austin, and J. Wilson (2008), The strength of the Brewer-Dobson circulation in a changing climate: coupled chemistry-climate model simulations, *J. Clim.*, *21*, 40–57.

Limpasuvan, V., and D. L. Hartmann (2000), Wave-maintained annular modes of climate variability, *J. Clim.*, *13*, 4414–4429.

Mahlman, J. D., J. P. Pinto, and L. J. Umscheid (1994), Transport, radiative, and dynamical effect of the Antarctic ozone hole: A GFDL "SKYHI" model experiment, *J. Atmos. Sci.*, *51*, 489–508.

Manzini, E., S. C. Bruhl, M. A. Giorgetta, and K. Kurger (2003), A new interactive chemistry-climate model: 2. Sensitivity of the middle atmosphere to ozone depletion and increase in greenhouse gas and implications for recent stratospheric cooling, *J. Geophys. Res.*, *108*(D14), 4429, doi:10.1029/2002JD002977.

Marshall, G. (2003), Trends in the southern annular modes from observations and reanalyses, *J. Clim.*, *16*, 4134–4143.

McLandress, C., and T. Shepherd (2009), Simulated anthropogenic changes in the Brewer-Dobson circulation, including its extension to high latitudes, *J. Clim*, *22*, 1516–1540.

Oman, L., D. W. Waugh, S. Pawson, R. S. Stolarski, and P. A. Newman (2009), On the influence of anthropogenic forcings on changes in the stratospheric mean age, *J. Geophys. Res.*, *114*(D3), D03105, doi:10.1029/2008JD010378.

Pawson, S., R. S. Stolarski, A. R. Douglass, P. A. Newman, J. E. Nielsen, S. M. Frith, and M. L. Gupta (2008), Goddard Earth Observing System chemistry-climate model simulations of stratosphere ozone-temperature coupling between 1950 and 2005, *J. Geophys. Res.*, *113*(D12), D12103, doi:10.1029/2007JD009511.

Perlwitz, J., S. Pawson, R. L. Fogt, J. E. Nielsen, and W. D. Neff (2008), Impacts of stratospheric ozone hole recovery on Antarctic climate, *Geophys. Res. Lett.*, *35*(8), L08714, doi:10.1029/2008GL033317.

Randel, W., and F. Wu (1999), Cooling of the Arctic and Antarctic polar stratosphere due to ozone depletion, *J. Clim*, *12*, 1467–1479.

Santer, B. D., T. M. L. Wigley, J. S. Boyle, D. J. Gaffen, J. J. Hnilo, D. Nychka, D. E. Parker, and K. E. Taylor (2000), Statistical significance of trends and trend differences in layer-average atmospheric temperature time series, *J. Geophys. Res.*, *105*(D6), 7337–7356.

Stolarski, R. S., A. R. Douglass, M. Gupta, P. A. Newman, S. Pawson, M. R. Schoeberl, and J. E. Nielsen (2006), An ozone increase in the Antarctic summer stratosphere: a dynamical response to the ozone hole, *Geophys. Res. Lett.*, *33*(21), L21805, doi:10.1029/2006GL026820.

Song, Y, and W. Robinson (2004), Dynamical mechanisms for stratospheric influence on the troposphere, *J. Atmos. Sci.*, *61*, 1711–1725.

Thompson, D. W. J., and J. M. Wallace (2000), Annular Modes in the extratropical circulation: Part I: month-to-month variability, *J. Clim.*, *13*, 1000–1016.

Thompson, D. W. J., and S. Solomon (2002), Interpretation of recent Southern Hemisphere climate change, *Science*, *296*, 895–899.

Thompson, D. W. J., J. M. Wallace, and G. C. Hegerl (2000), Annular Modes in the extratropical circulation: Part II: trends, *J. Clim.*, *13*, 1018–1036.

Thompson, D. W. J., M. P. Baldwin, and S. Solomon (2005), Stratosphere-troposphere coupling in the Southern Hemisphere, *J. Clim.*, *62*, 708–715.

Waugh, D. W., W. J. Randel, S. Pawson, P. A. Newman, and E. R. Nash (1999), Persistence of the lower stratospheric vortices, *J. Geophys. Res.*, *104*(D22), 27,191–27,201.

F. Li, Goddard Earth Sciences and Technology Center, University of Maryland Baltimore County, 5523 Research Park Drive, Suite 320, Baltimore, MD 21228, USA. (feng.li@nasa.gov)

P. A. Newman and R. S. Stolarski, Atmospheric Chemistry and Dynamics Branch, NASA Goddard Space Flight Center, Mail Code 613.3, Greenbelt, MD 20771, USA.